https://doi.org/10.17221/107/2019-JFS

Calculation of the aboveground carbon stocks with satellite data and statistical models integrated into the climatic parameters in the Alborz Mountain forests (northern Iran)

Mohadeseh Ghanbari Motlagh[1], Sasan Babaie Kafaky[1], Asadollah Mataji[1], Reza Akhavan[2]*

[1]Department of Forestry, Faculty of Natural Resources and Environment, Science and Research Branch, Islamic Azad University, Tehran, Iran

[2]Research Institute of Forests and Ranglands, Agricultural Research Education and Extension Organization (AREEO), Tehran, Iran

**Corresponding author: mohadeseh.motlagh@gmail.com*

Citation: Ghanbari Motlagh M., Kafaky S.B., Mataji A., Akhavan R. (2019): Calculation of the aboveground carbon stocks with satellite data and statistical models integrated into the climatic parameters in the Alborz Mountain forests (northern Iran). J. For. Sci., 65: 493–503.

Abstract: The forest ecosystems of northern Iran in the Alborz Mountains with a wide distribution range have variations in the composition and types of the plants, soil, structure, carbon stocks and climatic conditions. This study investigated the use of a satellite database and climatic parameters in estimating the carbon reserves. Three regions were selected for the distribution range of these forests. The data of 4 climatic parameters (MAP, MHR, MAE and MAT) were modelled based on the relationship with an elevation gradient. 5 spectral vegetation indices (*RVI*, *NDVI*, *SR*, *NDGI*, *DVI* and *TVI*) and near-infrared band (*NIR*) extracted from the satellite data and the aboveground carbon data of these forests were modelled based on a regression analysis. Finally, the best model of the relationship between the climate variables and the carbon stocks and the satellite indices was obtained from the multivariate linear regression equation and the R^2 coefficient. Accordingly, the most influential climatic parameters on the carbon stocks of these forests were precipitation, temperature, and also the most significant indices were *NDVI, RVI* and *NIR* band. This research is an attempt to model the calculations of the aboveground carbon in the forests of northern Iran in relation to the climatic parameters using satellite imagery.

Keywords: climate; carbon trees; broadleaf forests; spectral indices

The temperate deciduous broadleaf forests known as the Hyrcanian forests in northern Iran are the most important and valuable forest ecosystem in the vicinity of the world's largest lake (Caspian) (Siadati et al. 2010). Estimates have shown that the area of these forests was about 5 million hectares in the past, with the development of villages and the expansion of cities, converting the forested land into farmland and gardens, the grazing of livestock, deforestation, it has been steadily declining over the recent decades (Kalbi et al. 2014; Naqinezhad, Zarezadeh 2013). So, there are approximately 1.8 million hectares that remain today (Marvie-Mohadjer 2012; Hosseini 2010; Sagheb-Talebi et al. 2014). The distinction of these forests is that, as the remnants of the Tertiary period, in fact the last remnants of the world's natural broadleaf forests, they have species that are included in the fossils in Europe in that era (Akhani et al. 2010). Therefore, they are considered to be one of the richest and most unique forests in the world compared to their counterparts (Jafari et al. 2013). These forests are spread over three of the northern provinces of Iran (Gilan, Mazandaran and Golestan) on the northern slopes of the Alborz Mountains, 800 km long and up to 2,800 m above sea level (Sagheb-Talebi et al. 2014; Jourgholami, Majnounian

https://doi.org/10.17221/107/2019-JFS

2011). This wide geographic distribution range certainly has differences in the climate conditions, soil, site quality, species diversity and structure of these forests (Marvie-Mohadjer 2012). These forests are also subject to a range of diverse ecological conditions in the species and structure due to their mountainous nature and high-altitude expansion along the elevation gradient (Siadati et al. 2010).

Changes in the climatic parameters along the elevation gradient can affect many forest ecosystem characteristics such as the species composition, structure, biodiversity and carbon stocks of the vegetation and soil in mountain ecosystems (Zhu et al. 2010). Climatic factors affect the growth and distribution of plants as part of the site factors related to the atmosphere and the aboveground and underground parts, including the air temperature, solar radiation, air humidity, wind and atmospheric air pressure (Marvie-Mohadjer 2012). Hence, due to the mountainous extent and nature of these forests, it is important to understand the role of the environmental and climatic variables that control the distribution of the forest biomass and carbon. Much of the carbon stocks of nature is stored in the textures and bodies of the trees and the soil of the forests (Ardakani 2018). The forest biomass has captured the atmospheric carbon through photosynthesis for centuries (Dube, Mutanga 2016), which itself plays a role in the carbon cycle resistance and climate stability and in preventing global warming (Chen et al. 2019b; Vafaei et al. 2018). A large area of Iran consists of arid and semi-arid regions. According to the World Food Organization, the natural forest ecosystems in this country have been declining ever since 1990 (FAO 2015). The research by Faraji et al. (2015) have identified the forests of northern Iran as an important biomass storage through the aboveground biomass and one of the main carbon stocks of Iran. Therefore, calculating the amount of the carbon stocks in these forests is a necessity for both the conservation and mitigating the climate change as well as the release of carbon into the atmosphere.

Estimation of the carbon stored in the forests has been experimented with in different ways (Motlagh et al. 2018). The most widely applied procedures are ground measurement and surveying methods. However, it is time-consuming, costly and impractical for the mountain ecosystems because of the difficult physiographic and climatic conditions in these areas (Watson 2009; Sharifi et al. 2013; Kalbi et al. 2014). Recent technological advances such as arcGIS and remote sensing have provided researchers and planners with many opportunities (Mirajhorlou, Akhavan 2017; Poorzady, Bakhtiari 2009; Vafaei et al. 2018; Lu et al. 2016). Because of their unique characteristics, such as broad and integrated vision, high accuracy, time savings, cost, ease of access to information and repeatability, these methods have been valuable tools in recent decades for studying and monitoring the carbon stocks and forest biomass (Poorzady, Bakhtiari 2009; Zhu et al. 2015; Motlagh et al. 2018; Vafaei et al. 2018 Chen et al. 2019b; Van Pham et al. 2019).

So far, few studies have been conducted on the quantities and distribution of the forest biomass and carbon interfering with climate information with data from satellites (Baccini et al. 2004; Yin et al. 2015; Zhang et al. 2014; Dube, Mutanga 2016). In Iran, there has been no research on modelling the relationship between the forest biomass and the aboveground carbon (*AGC*) with climate variables. The only study, by Abdollahnejad et al. (2017), has investigared the relationship between the tree species distribution and the climatic parameters in the Golestan province, using the Quickbird satellite data. The aim of this study is to test and model the quantity of the carbon stocks in the forests of northern Iran by integrating the satellite data and climatic parameters.

MATERIAL AND METHODS

Study area

The forests of three watersheds were selected in the northern slopes of the Alborz Mountains in northern Iran: watershed number 84 in Golestan province, in the east, watershed number 38 in Mazandaran province in the centre and watershed number 7 in Gilan province, in the west (Fig. 1). The studied regions include the uneven structured broadleaf forests with *Fagus orientalis* and other species such as *Carpinus betulus*, Acer sp., *Diopyrus lotus*, *Cerasus avium*, Alnus sp., *Quercus castaneofolia*, *Tilia begonifolia*, *Parrotia persica*, Ulmus sp..

The sample plots of 900 m^2 were selected randomly. These sample plots were identified with arcGIS tools within the regions with a homogeneous slope (15–35%), the aspect (N, NE, NW) and in two elevation ranges, 500–800 m and 1,500–1,800 m (Table 1):

https://doi.org/10.17221/107/2019-JFS

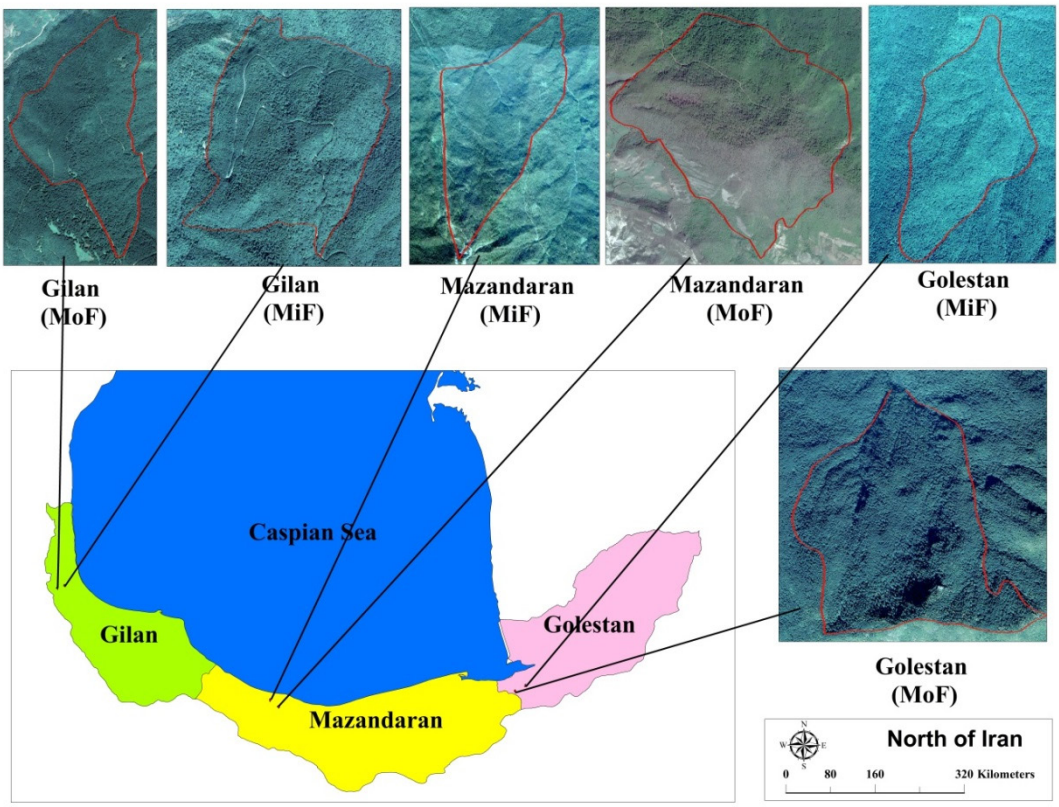

Fig 1. The location map of the study regions in northern Iran (MoF – mountain forest, MiF – midaltitude forest)

(*i*) Mountain forest (1,500–1,800 m) (MoF) and (*ii*) Midaltitude forest (500–800 m) (MiF).

Ground measurements and calculations of carbon stocks of trees

An important parameter for estimating the forest carbon stocks is the above-ground biomass (*AGB*) of standing trees (Chenge, Osho 2018; Chen et al. 2019a). For this purpose, variables such as the diameter at breast height (with a caliper to a millimeter in precision), the tree height (with a Suunto to a centimeter in precision), the crown diameters (with a tape to a meter in precision) were recorded for all the trees in the plot (Nyamugama, Kakembo 2015).

In the calculations using the measured variables of the trees, the calculation procedure of the tree biomass was performed according to the IPCC method (Ostadhashemi et al. 2014; IPCC 2003) (Eq. 1):

Table 1. The characteristics of the study regions and the results of the *AGC* values of the trees

Region	Study area	No	MAT (°C)	MAP (mm)	Soil type	Forest type	*N*/ha	*V*/ha (m^3)	*h*'(m)	*AGC* ± StDV (t)
Gilan	MiF	20	11–14	1,126	sandy-loam	mixed broadleaf	189.28	655.870	19.04	303.936 ± 121.28
	MoF	28	8–11	1,035	clay-loam	beech stand	196.11	770.287	20.16	373.720 ± 150.37
Mazandaran	MiF	24	12–16	925	loam	mixed broadleaf	100.46	426.820	21.3	157.311 ± 104.70
	MoF	32	11–13	890	clay-loam	beech stand	126.04	661.476	21.69	275.409 ± 93.91
Golestan	MiF	20	12–16	725	clay-loam	mixed broadleaf	102.33	355.017	18.63	133.948 ± 59.04
	MoF	20	8–14	695	silt-loam	beech stand	108.22	345.285	26.87	187.837 ± 68.16

MoF – montain forest, MiF – midaltitude forest, No – number of plots, MAT– Mean annual temperature (°C), MAP – Mean annual precipitation (mm), *N*/ha – number per ha, *V*/ha – mean volume per ha, *h*' – average height, *AGC* – above-ground carbon ($t \cdot ha^{-1}$), StDV – standard deviation

https://doi.org/10.17221/107/2019-JFS

$$TAGC = \left[V \times WD \times BEF_2\right] \times C \quad (1)$$

where:
TAGC – total above-ground carbon (t)
V – stem volume (m^3)
WD – wood density
BEF_2 – averaged biomass expansion factor for the broadleaf species (1.4).
C – carbon conversion factor (0.5)

The carbon factor (*C*) of 0.5 was designated as the general carbon factor for the tree. The wood specific density (*WD*) (g) was obtained by sampling the forest trees (Marshal et al. 2012).

The stem volume (*V*) was calculated based on Equations 2 and 3.

$$A_b = \frac{\pi}{4} \times dbh^2 \quad (2)$$

$$V = A_b \times h \times Kc \quad (3)$$

where:
A_b – basal area at the *dbh* (m^2)
dbh – diameter at breast height (m)
h – tree height (m)
Kc – averaged tree shape coefficient for the broadleaved species in northern Iran (0.5) (Zobeiry 2000).

A one-way ANOVA (analysis of variance) and Duncan's test was used to compare the *AGC* data between the regions and a *t*-test was used to compare the *AGC* between the two altitude ranges in the STATISTICA (SPSS).

Estimation of the above-ground carbon from remote sensing

SPOT-6 multispectral satellite data acquired in August 2016 were used. It corresponds to the date of the ground measurements. The SPOT imagery has 4 spectral bands: blue, green, red, and infrared with wavelengths of 0.519–0.454 μm, 0.587–0.527 μm, 0.694-0.624 μm and 0.880–0.756 μm, respectively, and a spatial resolution of 6 m. The panchromatic band with a wavelength of 0.745–0.450 μm has a spatial resolution of 1.5 m. The satellite sensor is called Naomi. This satellite is one of the high-resolution satellites and commercial Earth observation satellites built by the EADS Program Center, Astrium (Toulouse) is France and launched on September 6, 2012 from India's PSLV base (https://azercosmos.az/).

Before applying the images, their quality was evaluated for geometrical errors, radiometry and cloud spots. The images used in this study were cloudless. Also, these images were corrected by the service provider. However, to ensure that there were not any errors, the geometric correction of the images was performed with a number of ground control points and topographic maps of the areas. Geometric correction was undertaken in ENVI software (Harris Geospatial Solution).

Appropriate processes, such as calculating vegetation indices, using red and infrared bands are applied to infer the relationship between these data and the ground data (Kalbi et al. 2014). After the spectral processing, those equivalent values of the plots were extracted from the Vegetation Index (*VI*) and entered as independent variables in the modelling process. These indices included the Ratio Vegetation Index (*RVI*), Normalized Difference Vegetation Index (*NDVI*) Simple Ratio (*SR*), Normalized Difference Greenness Index (*NDGI*), Differential Vegetion Index (*DVI*) and Transformed Vegetation Index (*TVI*) as well as the near-infrared band (*NIR*) (Table 2). The modelling was performed by a stepwise linear multivariable regression to show the relationship between the *AGC* and the computational indices and the *NIR*. The validity of the regression models was evaluated using the root mean square error (*RMSE*) and the coefficient of determination (R^2) (Equation 4, 5).

$$R^2 = 1 - \frac{\sum_{i=1}^{N}\left(AGC - \hat{AGC}\right)^2}{\sum_{i=1}^{N}\left(AGC - \overline{AGC}\right)^2} \quad (4)$$

$$RMSE = \sqrt{\frac{\sum_{i=1}^{N}\left(\hat{AGC} - AGC\right)^2}{N}} \quad (5)$$

where:
AGC – observed value of aboveground carbon,
$\hat{AGC}$ – averaged value of aboveground carbon,
$\overline{AGC}$ – predicted observed value of aboveground carbon,
N – number of samples (Vafaei et al. 2018).

Regression modelling of the climate parameters

The climate variables considered in this study include the Mean Annual Precipitation (MAP)(mm),

https://doi.org/10.17221/107/2019-JFS

Table 2. The vegetation indices used in the study

Symbol	Vegetation Index name	Equation	Reference
RVI	Ratio Vegetation Index	*RED/NIR*	Jordan 1969
NDVI	Normalized Difference Vegetation Index	*(NIR − RED)/(NIR + RED)*	Rouse et al. 1974
SR	Simple Ratio	*NIR/RED*	Birth, McVey 1968
NDGI	Normalized Difference Greenness Index	*GREEN − RED/GREEN + RED*	Chamard et al. 1991
DVI	Differential Vegetion Index	*NIR − RED*	Tucker 1979
TVI	Transformed Vegetation Index	$\frac{(NDVI+0.5)}{\lvert NDVI+0.5\rvert}\sqrt{\lvert NDVI+0.5\rvert}$	Perry, Autenschlager 1984

RED − red multispectral band, *NIR* − near-infrared band, *GREEN* − red multispectral band

the Mean Annual Temperature (MAT)(C°), the Mean Relative Humidity (MRH)(%) and the Mean Annual Evaporation (MAE)(mm). They were obtained from the nearest meteorological rain stations within and around the study regions. Since the climatic stations were either scarce or non-existent in the high-altitude regions, the modelling was performed using a regression analysis (Farajzadeh 2015). In each region, and for each climate parameter, the types of regression equations (linear, exponential and polynomial) were constructed based on the altitude (gradient equation) in MS Excel (Microsoft). Then, the best equation was selected with the highest values of as the gradient equation of the climate parameter. In the next step, the best gradient equations were introduced into the arcGIS (ESRI). The climate parameter zoning maps for the study regions were constructed using digital elevation model (DEM) in arcGIS. Again, the values of the climatic parameters were extracted from the layers on the plots in the areas.

Pearson's correlation was used to investigate the relationship between the climate parameters and the independent variables – *VI*'s and the dependent variable – *AGC*. Finally, the stepwise multivariate linear regression analysis was used to find the best regression model. All the modelling and relationships of this section were made in STATISTICA (SPSS) and MS Excel (Microsoft).

RESULTS

Comparison of the above-ground carbon between the plots

The results of comparing the mean values of *AGC* using one-way ANOVA showed significant differences in *AGC* between the three regions, both elevation range MiF and MoF. There is an increasing trend from east to west ($P \leq 0.05$) (Table 1 and 3). Also, the results of *t*-test *AGC* indicated that there were significant differences between the *AGC* values in the two elevation ranges in all three regions. *AGC* of MoF is bigger than MiF (Table 4) ($P \leq 0.05$).

Table 3. The results of the *AGC* variation analysis in the study regions

Carbon Stock Source		Sum of Squares	*df*	Mean Square	*F*	*P*
AGC	(MoF)	218933.613	2	109461.807	13.151	0.000**
	(MiF)	187170.070	2	93585.035	17.638	0.000**

MoF – montain forest, MiF – midaltitude forest, *df* – degrees of freedom, *F* – Fisher's test, *P* – probability, ** significant at level 99%

Table 4. The *T*-test results of the *AGC* between the two elevation ranges in the study regions

Region	Carbon Stock Source	Mean Difference	*df*	*F*	*t*	*P*
Gilan	*AGC*	48.92317	46	2.295	1.490	0.0143
Mazandaran	*AGC*	86.76323	54	1.763	4.622	0.000**
Golestan	*AGC*	41.16643	38	0.017	2.222	0.033*

AGC – aboveground carbon, *df* – degrees of freedom, *P* – probability, *F* – Fisher's test, *t* – Student's test, *significant at level 95%, ** significant at level 99%

https://doi.org/10.17221/107/2019-JFS

Table 5. The climatic equations used in the climate map in the study regions

Region	Equation	R^2	Model
Gilan	MAT = –0.004x + 16.13	0.988	linear
	MAP = 0.0006 –1.089x + 1324.40	0.797	polynomial
	MRH = –0.0061x + 78.77	0.661	linear
	MAE = 0.3088x + 775.21	0.994	linear
Mazandaran	MAT = –0.0032x + 16.79	0.973	linear
	MAP = 0.0002–0.612x + 1094.50	0.981	polynomial
	MRH = –0.00114x + 83.11	0.773	linear
	MAE = –0.0004 + 0.569x + 978.73	0.711	polynomial
Golestan	MAT = –0.0036x + 18.57	0.834	linear
	MAP = 4E– 0.7 – 0.499x + 631.03	0.319	polynomial
	MRH = –0.009x + 71.92	0.783	linear
	MAE = 0.002 + 0.546x + 922.67	0.697	polynomial

MAT – mean annual temperature (C°), MAP – mean annual precipitation (mm), MRH – mean relative humidity (%), MAE – mean annual evaporation (mm), x – altitude, R^2 – coefficient of determination

Results of the climatic information

The selected gradient equations for each of the climate parameters are presented in Table 5. In the equations, *y* is the value of the climatic parameter and *x* is the altitude.

The relationship between the temperature and humidity with the altitude in all three study regions was a linear inverse relationship with the increasing altitude, these two parameters showed a decreasing trend. The relation of the MAP with the altitude is a polynomial relationship with the increasing altitude to a certain altitude which initially has a decreasing trend after which we can see an increasing trend. The MAE parameter in Gilan has an increasing linear relationship with the altitude, while, in the other two regions, it has an upward trend to a certain altitude, followed by a downward trend.

The results of estimating the above-ground carbon from the satellite data

The best regression model between the *AGC* values and indices and the *NIR* band in the study areas was the linear relationship among which the models with the highest R^2 and the lowest RMSE were selected as the most appropriate models. The relationship between the *NDVI, TVI, NDGI, DVI* and *NIR* band with the *AGC* was a significant positive relationship, but this relationship was the inverse for the *RVI* and *SR*. Among the studied indices, the *NDVI*, *RVI* and *NIR* bands showed the highest significant level and the highest R^2 and the lowest RMSE in all the regions. These indices and *NIR* bands were the best predictors of the *AGC* model in the study areas. The single and multivariable regression models were constructed between the the values of the *AGC* based on the plots as the dependent variable and the indices as the independent variable. The models with the highest R^2 are listed in Table 6.

Modelling the relationship between the climate parameters and the indices with the above-ground carbon

At this stage, the climatic parameters and vegetation indices achieved from the models made in the previous section were entered into a multiple linear regression model to finally select the computational model with the highest R^2 (Table 7). The best model presented for modelling the relationship between the climate parameters and the vegetation indices and the *AGC* values in Gilan shows that the MAP, MAT, *NIR* band and *NDVI* are the best predictors of the model. In Mazandaran, the MAP and *RVI* are the best predictors, and, finally, in Golestan province, the best predictors of the model are shown for the *AGC* with the MAT and *NDVI*.

https://doi.org/10.17221/107/2019-JFS

Table 6. The most favourable estimation models obtained from the single and multivariable regression analysis between the above-ground carbon (*AGC* in t) and the indices and the bands used in the study

Region		Regression equation	R^2	*RMSE* (t·ha^{-1})
Gilan	MoF	*AGC* = 123.88 + 5.35 (*NDVI*) + 0.0003 (*NIR*) – 8.25 (*RVI*)	0.60	0.19
	MiF	*AGC* = 100.41 + 2.37 (*NDVI*) + 0.01 (*NIR*)	0.63	0.21
Mazandaran	MoF	*AGC* = 78.36 + 8.982 (*NDVI*)– 9.22 (*RVI*)	0.66	0.52
	MiF	*AGC* = 69.01 + 5.57 (*NDVI*) + 0.07 (*NIR*)	0.66	0.88
Golestan	MoF	*AGC* = 23.669 + 3.741 (*NDVI*) + 6.488 (*NIR*)	0.71	0.09
	MiF	*AGC* = 18.21 + 2.09 (*NDVI*) + 7.09 (*NIR*)	0.69	0.14

MoF – montain forest, MiF – midaltitude forest, *AGC* – aboveground carbon, *NDVI* – Normalized Difference Vegetation Index, *NIR* – near-infrared band, *RVI* – Ratio Vegetation Index, R^2 – coefficient of determination, *RMSE* – root mean square error

Table 7. Modelling the *AGC* values with the integration of the climate parameters and the spectral indices

Region	Model	R^2	*RMSE* (t·ha^{-1})
Gilan	*AGC* = 0.68 (MAP) – 3.188 (MAT) + 412.262 (*NDVI*) – 27.676 (*NIR*) + 127.330	0.619	15.23
Mazandaran	*AGC* = –0.059 (MAP) – 2.437 (*RVI*) + 113.098	0.706	13.88
Golestan	*AGC* = –2.261 (MAT) – 0.041 (*NDVI*) – 77.597	0.664	17.45

AGC – aboveground carbon, MAP – mean annual precipitation (mm), MAT – mean annual temperature (C°), *NDVI* – Normalized Difference Vegetation Index, *NIR* – near-infrared band, *RVI* – Ratio Vegetation Index, R^2 – coefficient of determination, *RMSE* – root mean square error

DISCUSSION AND CONCLUSION

In this study, the *AGC* was estimated at two elevation ranges, namely, the MoF and MiF and along the northern slopes of the Alborz Mountains in three regions in northern Iran. Based on the results of the calculations, the estimated *AGC* was significantly bigger than the mountain elevations and from east to west.

The general trend of the climatic parameters in all three study regions, based on the regression and output equations of the models in GIS, is that by increasing the altitude, the mean temperature decreases, but the precipitation decreases to a certain height and then there is an increasing trend. The relative humidity has also decreased with the rising altitude in all three provinces where these forests are present in the Alborz Mountains. Evaporation in Guilan showed a linear upward trend and in the other two regions initially increased with a peak at 800 m and 1200 m, respectively, for Mazandaran and Golestan and then decreased.

There is a basic difference between the eastern and western parts of the Hyrcanian forests in terms of the precipitation and temperature. So that the highest amount of rainfall and humidity was observed in the western part (Gilan) and, in contrast, the highest MAT and drought period in the eastern part (Golestan), which, in turn, caused changes in the environmental conditions, structural changes, species diversity and lead to variations in the forest biomass and carbon (Akhani et al. 2010; Jourgholami, Majnounian 2011; Kalbi et al. 2014).

Previous studies in the northern forests of Iran have noted the significant fluctuations in the density and growth rate and biodiversity of these forests from east to west (Jafari et al. 2013; Motlagh et al. 2018; Siadati et al. 2013; Mirajhorlou, Akhavan 2017; Akhani et al. 2010). Different findings have always been achieved in this type of study, which could be due to human interference, heterogeneity in the microclimate, soil and topography. Also, based on the results obtained in the present study, there is an increase in the *AGC* in these forests despite the decreasing temperatures. With an increasing altitude, the temperature decreases. Because the photosynthetic activity relies on the temperature, it also has an effect on the *AGB* and *AGC* (Alvarez-Davila et al. 2017). Photosynthesis increases slightly with an increasing temperature, but, on the other hand, it increases the respiration which, with high humidity, causes a sultry state at lower altitudes (Rana et al. 1989). However, at the local and regional scales, the biomass and carbon

https://doi.org/10.17221/107/2019-JFS

values are affected by a large number of variables. The present results can be attributed to the relatively higher soil fertility of the forest sites in the high land. In addition, the tree density, tree height, and basal area are important predictive parameters for estimating the carbon stocks, which in this study have been influential in the results obtained.

Based on the strongest regression models in this study, the most important variables predicting the *AGC* in Gilan were the MAP, MAT, near-infrared band and the *NDVI*. In Mazandaran, the MAP and the *RVI* in relation to the carbon stocks of the forests in this region have created the most favourable predictive model and in Golestan province, the MAT parameter and *NDVI* were the best parameters. In the final regression equations made in all three zones, the two factors of precipitation and temperature showed the strongest relationship with the highest values of the coefficient of determination with the *AGC*.

This indicates that, in general, these two factors are the main climatic factors controlling the *AGC* in the forests of northern Iran. The results of two indices of the *NDVI*, *RVI* and near-infrared band (*NIR*) are suggested to be the best variables in estimating the carbon stocks of the broadleaf deciduous trees in northern Iran. These computational vegetation indices are sensitive to the photosynthetic parts of the vegetation through the optical images (Yan et al. 2013).

On the other hand, the multivariable regression analysis has been used as one of the empirical modelling methods in most studies to estimate the quantitative characteristics such as the carbon stocks of the trees (Nyamugama, Kakembo 2015; Baccini et al. 2004). In Gilan and Mazandaran, the multivariable linear regression models with the *NDVI*, *RVI* and *NIR* and in Golestan, the *NDVI* and *NIR* regression models were selected as the best multivariate relationships for estimating the forest *AGC*.

Several studies have concluded that adding satellite spectral information in combination with environmental information can improve the prediction of the qualitative and quantitative characteristics of the forests. Among the results of Abdollahnejad et al. (2017), the study in the forests of Golestan province in northern Iran showed that in modelling the tree species diversity with the QuickBird data and environmental parameters, the temperature and then the precipitation were significant variables. Also, the findings of Luther et al. (2002) have shown that biomass models improve the biomass estimations when developed as a function of remote sensing variables in combination with the environmental characteristics including the moisture index, precipitation, growth period and digital elevation model. Baccini et al. (2004) examined the forest biomass across the national forests in California, USA, using MODIS information, the annual precipitation, the annual temperature, altitude information and statistical models. The results showed that the MODIS data in combination with the topography and climate can be used to produce

AGB maps with good accuracy across these regions. Dube and Mutanga (2016) used a database of WorldView2 with environmental variables of radiation, temperature, soil moisture coefficient, elevation, slope and aspect to estimate the biomass and carbon in a natural forest and a planted forest in South Africa. The results showed that the integration of the spectral indices and data bands with the climatic variables improved the *AGB* and *AGC* estimates and provided a robust tool for the accurate and reliable estimation of the *AGB* and *AGC* stocks in the forest ecosystems.

One of the major challenges in the results of the studies focused on the integration of the climate and satellite variables in estimating the *AGB* and *AGC* in the forests can be the low accuracy of the biomass and carbon values, the estimates due to the low spatial resolution of the images, the effects of human activities, the previous climate, the study scale, etc. has been noted (Yin et al. 2015; Dube, Mutanga 2016; Nyamugama, Kakembo 2015; Zhang et al. 2014; Baccini et al. 2004).

Since the estimation and mapping of these parameters is essential for efficient forest management and their role in the global carbon cycle, researchers who combine multispectral imagery with a spatial resolution of 10 meters and above with the environmental variables which can estimate the quantification and mapping of important structural properties of the forests are more successful (Dube, Mutanga 2016; Chen et al. 2019a). In this study, the satellite images used have this capability.

The reasons for the dissatisfaction of some of the results of the indices used in this study can be attributed to the mixed nature of the forests, the multilayered forest stands and the mountain pro-

https://doi.org/10.17221/107/2019-JFS

file of the Hyrcanian forests and the existence of a variety of error sources (Kalbi et al. 2014). However, the use of multivariable methods in Plant Biological Climate Research has the potential to dramatically reduce the primary variables to several limiting and measurable factors in the distribution of the forest carbon stocks (Yin et al. 2015).

The research is an attempt to model the calculations of the *AGC* in the Hyrcanian forests in northern Iran in relation to the climatic parameters using satellite imagery. The results of this study demonstrate the effectiveness of the multivariable statistical methods in modelling the severity of the effect of the climate factors on the distribution of the forest carbon stocks. The results also illustrated that the carbon stocks were the most sensitive to the two factors of the mean temperature and the mean precipitation.

In remote sensing estimations, in order to quickly and reliably estimate the carbon of the trees in these forests, based on the results of this study, the vegetation indices of the *NDVI*, *RVI* and near-infrared band (*NIR*) are recommended as the most desirable predictor variables to reduce the estimation costs.

Finally, due to the high extent of the distribution of these forests, it is suggested that the interactions between the carbon stocks of the different forest communities and species with the factors such as the soil and geological structures should be investigated and entered into a database for modelling it in order to manage and protect these valuable forests.

Rererences

Abdollahnejad A., Panagiotidis D., Joybari S.S., Surový P. (2017): Prediction of Dominant Forest Tree Species Using QuickBird and Environmental Data. MDPI AG. Forests, 8: 19.

Akhani H., Djamali M., Ghorbanalizadeh A. Ramezani, E. (2010): Plant biodiversity of Hyrcanian relict forests, N Iran: an overview of the flora, vegetation, palaeoecology and conservation. Pakistan Journal of Botany, 42: 231–258.

Álvarez-Dávila E., Cayuela L., González-Caro S., Aldana A.M., Stevenson P.R., Phillips O., Cogollo Á., Peñuela M.C., von Hildebrand P., Jiménez E. Melo O., Londoño-Vega A.C., Mendoza I., Velásquez O., Fernández F., Serna M., Velázquez-Rua C., Benítez D., Rey-Benayas J.M. (2017): Forest biomass density across large climate gradients in northern South America is related to water availability but not with temperature. PloS One,12: e0171072.

Ardakani M.R. (2018): Ecology. Tehran, Tehran University: 340. (in Persian)

Baccini A., Friedl M.A., Woodcock C.E. Warbington R. (2004): Forest biomass estimation over regional scales using multisource data. Geophysical research letters, 31: 4.

Birth G.S. and McVey G.R. (1968): Measuring the Color of Growing Turf with a Reflectance Spectrophotometer 1. Agronomy Journal, 60: 640–643.

Chamard P., Courel M.F., Ducousso M., Guénégou M.C., Le Rhun J., Levasseur J.E., Loisel C., Togola M. (1991): Utilisation des bandes spectrales du vert et du rouge pour une meilleure **évaluation** des formations végétales actives. Télédétection et Cartographie, Presses de l'Universite de Quebec, Montreal; Canada, AUPELF-UREF: 203–209.

Chen L., Wangc Y., Ren C., Zhang B., Wang Z. (2019a): Assessment of multi-wavelength SAR and multispectral instrument data for forest aboveground biomass mapping using random forest kriging. Forest Ecology and Management, 447: 12–25.

Chen L., Wang Y., Ren C., Zhang B. Wang Z. (2019b): Optimal Combination of Predictors and Algorithms for Forest Above-Ground Biomass Mapping from Sentinel and SRTM Data. Remote Sensing, 11: 414.

Chenge I.B., Osho J.S., (2018): Mapping tree aboveground biomass and carbon in Omo Forest Reserve Nigeria using Landsat 8 OLI data. Southern Forests: A Journal of Forest Science, 80: 341–350.

Dube T., Mutanga O. (2016): The impact of integrating World-View-2 sensor and environmental variables in estimating plantation forest species aboveground biomass and carbon stocks in uMgeni Catchment, South Africa. ISPRS Journal of Photogrammetry and Remote Sensing, 119: 415–425.

FAO (2015): Global Forest Resources Assessment, how are the world's forests changing? Second edition. Food and Agriculture Organization of the United Nations, Rome: 54.

Faraji F., Mataji A., Babaei Kafaki S., Vahedi A.A. (2015): The relationship between plant diversity and above-ground biomass changes in Fagus orientalis L. forests (Case study: Hajikola-Tirankoli, Sari). Iranian Forest Journal, Iranian Forestry Association. 7: 151–165. (in Persian)

Farajzadeh M. (2015): Climatology techniques. Publishing of Organization for the Study and Compilation of Humanities Books of Universities: 288.

Hosseini S.M. (2010): Forest operations management and timber products in the Hyrcanian forests of Iran. FORMEC in Forest engineering: Meeting the needs of the society and the environment, July 11 – 14, 2010, Padova – Italy: 11–14.

IPCC (2003): Good Practice Guidance for Land Use, Land-Use Change and Forestry (GPG-LULUCF). Available at: https://www.ipcc-nggip.iges.or.jp/public/gpglulucf/gpglulucf.htm

Jafari S.M., Zarre S. Alavipanah S.K. (2013): Woody species diversity and forest structure from lowland to montane

https://doi.org/10.17221/107/2019-JFS

forest in Hyrcanian forest ecoregion. Journal of Mountain Science, 10: 609–620.

Jordan C.F. (1969): Derivation of leaf-area index from quality of light on the forest floor. Ecology, 50: 663–666.

Jourgholami M. and Majnounian B. (2011): Harvesting systems in Hyrcanian forest, Iran; limitations and approaches. The forest engineering network (Formec, Austria, Proceedings) October: 9–13.

Kalbi S., Fallah A., Shataee SH. (2014): Estimation of forest attributes in the Hyrcanian forests, comparison of advanced space-borne thermal emission and reflection radiometer and satellite poure l'observation de la terre-high resolution grounding data by multiple linear, and classification and regression tree regression models. Journal of Applied Remote Sensing, 8: 083632 (2014).

Lu D., Chen Q., Wang G., Liu L., Li G., Moran E. (2016): A survey of remote sensing-based aboveground biomass estimation methods in forest ecosystems. International Journal of Digital Earth, 9: 63–105.

Luther J.E., Fournier R.A., Hall R.J., Ung C.H., Guindon L., Piercey D.E., Lambert M.C. Beaudoin A. (2002): A strategy for mapping Canada's forest biomass with Landsat TM imagery. In Geoscience and Remote Sensing Symposium, 2002. IGARSS'02. IEEE International, 3: 1312–1315.

Marshall A.R., Willcock S., Platts P.J., Lovett J.C., Balmford A., Burgess N.D., Latham J.E., Munishi P.K.T., Salter R., Shirima D.D., Lewis S.L. (2012): Measuring and modelling above-ground carbon and tree allometry along a tropical elevation gradient. Journal of Biological Conservation, 154: 20–33.

Marvie-Mohadjer M.R. (2012): Silviculture. Tehran, University of Tehran Press: 400.

Mirajhorlou K., Akhavan R. (2017): Forest density and orchard classification in Hyrcanian forests of Iran using Landsat 8 data. Journal of Forest Science, 63: 355–362.

Motlagh M.G., Kafaky S.B., Mataji A., Akhavan R. (2018): Estimating and mapping forest biomass using regression models and Spot-6 images (case study: Hyrcanian forests of north of Iran). Environmental Monitoring and Assessment, 190: 352.

Naqinezhad A., Zarezadeh S. (2013): A contribution to flora, life form and chorology of plants in Noor and Sisangan lowland forests. Journal of Taxonomy and Biosistematics, 4: 31–44.

Nyamugama A., Kakembo V. (2015): Estimation and monitoring of aboveground carbon stocks using spatial technology. South African Journal of Science, 111: 7.

Ostadhashemi R., Rostami Shahraji T., Roehle H., Mohammadi Limaei S. (2014): Estimation of biomass and carbon storage of tree plantations in northern Iran. Journal of Forest Science, 60: 363–371.

Perry C.R., Lautenschlager L.F. (1984): Functional equivalence of spectral vegetation indices. Journal of Remote Sensing of Environment. 14: 169–182.

Poorzady M., Bakhtiari F. (2009): Spatial and temporal changes of Hyrcanian forest in Iran. iForest-Biogeosciences and Forestry, 2: 198.

Rana B.S., Singh S.P. Singh R.P. (1989): Biomass and net primary productivity in Central Himalayan forests along an altitudinal gradient. Forest ecology and management, 27: 199–218.

Rouse Jr.J., Haas R.H., Schell J.A., Deering D.W. (1974): Monitoring vegetation systems in the Great Plains with ERTS. Third Earth Resources Technology Satellite-1 Symposium. I: NASA, Washington, DC: 309–317.

Sagheb-Talebi K., Sajedi T. Pourhashemi M. (2014): Forests of Iran: A Treasure from the Past, a Hope for the Future, 10: 39–151.

Sharifi A., Amini J. Pourshakouri F. (2013): Allometric Model Development for Above-Ground Biomass Estimation in Hyrcanian Forests of Iran. World Applied Sciences Journal, 28: 1322–1330.

Siadati S., Moradi H., Attar F., Etemad V., Hamzeh'ee B.E.H.N.A.M. Naqinezhad A., (2010): Botanical diversity of Hyrcanian forests; a case study of a transect in the Kheyrud protected lowland mountain forests in northern Iran. Phytotaxa, 7: 1–18.

Tucker C.J. (1979): Red and photographic infrared linear combinations for monitoring vegetation. Journal of remote sensing of Environment. 8: 127–150.

Vafaei S., Soosani J., Adeli K., Fadaei H., Naghavi H., Pham T. Tien Bui D. (2018): Improving accuracy estimation of forest aboveground biomass based on incorporation of ALOS-2 PALSAR-2 and sentinel-2A imagery and machine learning: A case study of the Hyrcanian forest area (Iran). Remote Sensing, 10: 172:

Van Pham M., Pham T.M., Du Q.V.V., Bui Q.T., Van Tran A., Pham H.M., Nguyen T.N. (2019): Integrating Sentinel-1A SAR data and GIS to estimate aboveground biomass and carbon accumulation for tropical forest types in Thuan Chau district, Vietnam. Remote Sensing Applications: Society and Environment, 14: 148–157.

Watson C. (2009). Forest carbon accounting: overview and principles. Forest Carbon Accounting: Overview and Principles: 39.

Yan F., Wu B., Wang Y. (2013): Estimating aboveground biomass in Mu Us Sandy Land using Landsat spectral derived vegetation indices over the past 30 years. Journal of Arid Land. 5: 521–530.

Yin G., Zhang Y., Sun Y., Wang T., Zeng Z., Piao S. (2015): MODIS based estimation of forest aboveground biomass in China. PloS One, 10: e0130143.

https://doi.org/10.17221/107/2019-JFS

Zhang J., Huang S., Hogg E.H., Lieffers V., Qin Y., He F. (2014): Estimating spatial variation in Alberta forest biomass from a combination of forest inventory and remote sensing data. Biogeosciences. 11: 2793–2808

Zhu B., Wang X., Fang W., Piao S., Shen H., Zhao S., Peng C. (2010): Altitudinal changes in a carbon storage of temperate forests on Mt Changbai, Northeast China. Journal of Plant Research, 123: 439–452.

Zhu Y., Liu K., Liu L., Wang S., Liu H. (2015): Retrieval of mangrove aboveground biomass at the individual species level with WorldView-2 images. Journal of Remote Sensing, 7: 12192–12214.

Zobeiry M. (2000): Forest Inventory (measurement of tree and stand). Tehran, Tehran University Publication: 401.

Received for publication September 3, 2019
Accepted after corrections December 3, 2019